

# Matched Filter Bounds for Reduced-Order Multichannel Models

Dirk T.M. Slock and Elisabeth De Carvalho  
 Institut EURECOM, 2229 route des Crêtes, B.P. 193,  
 06904 Sophia Antipolis Cedex, FRANCE  
 Tel: +33 93002606 Fax: +33 93002627  
 email:{slock,carvalho}@eurecom.fr

## ABSTRACT

We propose two Matched Filter Bounds (MFBs) to characterize the performance of receivers using reduced-order channel models. The first one (WMFB) uses the channel model to perform the spatio-temporal matched filtering that yields data reduction from multichannel to single-channel form. The rest of the processing remains optimal. The second one (ICMFB) on the other hand bounds the performance of the Viterbi algorithm with the reduced channel model. Two methods of obtaining reduced-order channel models are discussed to illustrate these measures: blind channel estimation by Deterministic Maximum Likelihood (which maximizes WMFB) and channel estimation by training sequence.

## 1 Introduction

We consider here a FIR Multichannel model. The multiple FIR channels are due to oversampling of a single received signal and/or the availability of multiple received signals from an array of antennas (in the context of mobile digital communications). To further develop the case of oversampling, consider linear digital modulation over a linear channel with additive noise so that the cyclostationary received signal can be written as

$$y(t) = \sum_k h(t - kT)a(k) + v(t) \quad (1)$$

where the  $a(k)$  are the transmitted symbols,  $T$  is the symbol period and  $h(t)$  is the channel impulse response. The channel is assumed to be FIR with duration  $NT$  (approximately). If the received signal is oversampled at the rate  $\frac{m}{T}$  (or if  $m$  different received signals are captured by  $m$  sensors every  $T$  seconds, or a combination of both), the discrete input-output relationship can be written as:

$$\mathbf{y}(k) = \sum_{i=0}^{N-1} \mathbf{h}(i)a(k-i) + \mathbf{v}(k) = \mathbf{H}A_N(k) + \mathbf{v}(k),$$

$$\mathbf{y}(k) = \begin{bmatrix} y_1(k) \\ \vdots \\ y_m(k) \end{bmatrix}, \mathbf{v}(k) = \begin{bmatrix} v_1(k) \\ \vdots \\ v_m(k) \end{bmatrix}, \mathbf{h}(k) = \begin{bmatrix} h_1(k) \\ \vdots \\ h_m(k) \end{bmatrix}$$

$$\mathbf{H} = [\mathbf{h}(N-1) \cdots \mathbf{h}(0)], A_N(k) = [a^H(k-N+1) \cdots a^H(k)]^H \quad (2)$$

where the subscript  $i$  denotes the  $i^{\text{th}}$  channel and superscript  $H$  denotes Hermitian transpose. In the case of oversampling,  $y_i(k)$ ,  $i = 1, \dots, m$  represents the  $m$  phases of the polyphase representation of the oversampled signal:  $y_i(k) = y(t_0 + (k + \frac{i}{m})T)$ . In the polyphase representation of the oversampled signals, we get a discrete-time circuit in which the sampling rate is the symbol rate. Its output is a vector signal corresponding to a SIMO (Single Input Multiple Output) or vector channel consisting of  $m$  SISO discrete-time channels where  $m$  is the sum of the oversampling factors used for the possibly multiple antenna signals. Let  $\mathbf{H}(z) = \sum_{i=0}^{N-1} \mathbf{h}(i)z^{-i} = [\mathbf{H}_1^H(z) \cdots \mathbf{H}_m^H(z)]^H$  be the SIMO channel transfer function. Consider additive independent white Gaussian noise  $\mathbf{v}(k)$  with  $r\mathbf{v}\mathbf{v}^H(k-i) = \mathbf{E} \mathbf{v}(k)\mathbf{v}^H(i) = \sigma_v^2 I_m \delta_{ki}$ . Assume we receive  $M$  samples:

$$\mathbf{Y}_M(k) = \mathcal{T}_M(\mathbf{H}) A_{M+N-1}(k) + \mathbf{V}_M(k) \quad (3)$$

where  $\mathbf{Y}_M(k) = [\mathbf{y}^H(k-M+1) \cdots \mathbf{y}^H(k)]^H$  and similarly for  $\mathbf{V}_M(k)$ , and  $\mathcal{T}_M(\mathbf{H})$  is a block Toeplitz matrix with  $M$  block rows and  $[\mathbf{H} \ 0_{m \times (M-1)}]$  as first block row.

The classical Matched Filter Bound (MFB) indicates the optimal symbol detection performance when the channel is perfectly known. In section 2 of this paper, we present four different ways of interpreting this MFB in the multichannel case. In practice, the channel impulse response length we can afford to estimate is often shorter than the true channel length. Therefore, in section 3, we define two appropriate MFBs when a reduced-order channel model is used. At last, in section 4, two methods for obtaining reduced-order channel models are presented to illustrate the two MFBs: blind Deterministic Maximum Likelihood estimation, and training sequence based estimation.

## 2 Different Matched Filter Bound Definitions

### 2.1 Continuous Processing MFB

We present here four different ways of computing the MFB in the case of continuous transmission, for the multichannel  $\mathbf{H}(z)$ , shown in Fig. 1, where the input symbols  $a(k)$  are white and the additive noise  $\mathbf{v}(k)$  is temporally and spatially white. We introduced the following notation for the matched filter:  $\mathbf{H}^\dagger(z) = \mathbf{H}^H(1/z^*)$ .

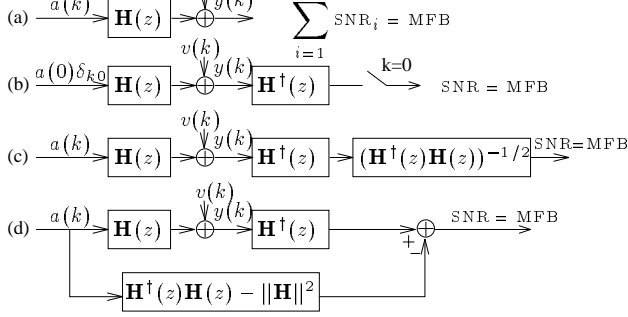


Figure 1: Four Interpretations for the Continuous Processing MFB from SNRs.

The MFB can alternatively be calculated as the sum of the SNRs in the individual channels in (a), as the SNR of the appropriate output sample of the matched filter (MF) when transmitting only one symbol in (b), as the SNR of the output of the whitened MF (WMF) in (c) or finally as the SNR at the output of the MF from which past and future symbol contributions (ISI) are eliminated. The MFB, calculated from (a), (b), (c) or (d), is equal to  $\|\mathbf{H}\|^2 \sigma_a^2 / \sigma_v^2$ .

## 2.2 Burst Processing MFB

The MFB becomes symbol-dependent in the case of burst (packet) transmission. Suppose we transmit the burst  $A_{M+N-1}(k)$ . According to equation (3), the corresponding multichannel output is:  $\mathbf{Y}_M(k) = \mathcal{T}_M(\mathbf{H}) A_{M+N-1}(k) + \mathbf{V}_M(k)$ . In the different structures presented in Fig. 1, the multichannel  $\mathbf{H}(z)$  is replaced by the filtering matrix  $\mathcal{T}_M(\mathbf{H})$  in the time-domain, and the burst multichannel matched filter becomes  $\mathcal{T}_M^H(\mathbf{H})$ . Since the MFB is symbol-dependent, we shall in fact consider the average MFB over the symbols in the burst. In a burst context, Fig. 1(b) is no longer of interest, this is why we will not consider this configuration anymore.

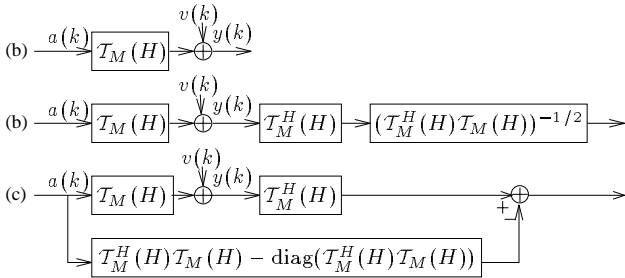


Figure 2: Four ways to get the Burst MFB from SNRs.

In Fig. 2(a), the burst signal covariance matrix at the channel output is:  $\sigma_a^2 \mathcal{T}_M(\mathbf{H}) \mathcal{T}_M^H(\mathbf{H})$ . The noise variance is  $\sigma_v^2 I$ . The SNR for the  $i^{\text{th}}$  element of the output is then:

$$SNR_i^{(a)} = \frac{\sigma_a^2 (\mathcal{T}_M(\mathbf{H}) \mathcal{T}_M^H(\mathbf{H}))_{i,i}}{\sigma_v^2} \quad (4)$$

$$SNR_i^{(b)} = \frac{\sigma_a^2 [(\mathcal{T}_M^H(\mathbf{H}) \mathcal{T}_M(\mathbf{H}))^{H/2} (\mathcal{T}_M^H(\mathbf{H}) \mathcal{T}_M(\mathbf{H}))^{1/2}]_{i,i}}{\sigma_v^2} \quad (5)$$

The signal component is  $\text{diag}(\mathcal{T}_M^H(\mathbf{H}) \mathcal{T}_M(\mathbf{H})) A_{M+N-1}(k)$  in (c) (where  $\text{diag}(\cdot)$  denotes a diagonal matrix containing of the main diagonal of its argument), hence its variance,  $\sigma_a^2 (\mathcal{T}_M^H(\mathbf{H}) \mathcal{T}_M(\mathbf{H}))_{i,i}^2$ , for the  $i^{\text{th}}$  element, for which the noise variance is  $\sigma_v^2 (\mathcal{T}_M^H(\mathbf{H}) \mathcal{T}_M(\mathbf{H}))_{i,i}$ . Thus we find:

$$SNR_i^{(c)} = \frac{\sigma_a^2 (\mathcal{T}_M^H(\mathbf{H}) \mathcal{T}_M(\mathbf{H}))_{i,i}}{\sigma_v^2} \quad (6)$$

Hence, we find the following equivalent expressions:

$$\sum_{i=1}^{Mm} SNR_i^{(a)} = \sum_{i=1}^{M+N-1} SNR_i^{(b)} = \sum_{i=1}^{M+N-1} SNR_i^{(c)}. \quad (7)$$

The structure in Fig. 1(a) represents in fact a different point of view from (b) or (c). Indeed, the  $M+N-1$  outputs of (b) and (c) are directly related to the  $M+N-1$  input samples; in (a) we get  $Mm$  output samples. The measure in equation (7) can then be taken as a measure of the Burst MFB. This leads to the following average MFB per symbol.

$$\begin{aligned} MFB &= \frac{1}{M+N-1} \sum_{i=1}^{Mm} SNR_i^{(a)} \\ &= \frac{1}{M+N-1} \sum_{i=1}^{M+N-1} SNR_i^{(b)} = \frac{1}{M+N-1} \sum_{i=1}^{M+N-1} SNR_i^{(c)} \end{aligned} \quad (8)$$

Note that, as the length of the burst grows to infinity, the average MFB over the burst converges to the continuous processing MFB. For structures (b) and (c) this follows from the fact that the MFB in the middle of the burst converges to the continuous processing MFB.

## 3 Matched Filter Bounds for Reduced-Order Models

The MFB computation considered in the previous section requires knowledge of the channel. However, in channel estimation, a channel order misestimation may happen. Since physical channel impulse responses tend to be of infinite length, this misestimation will often mean an underestimation. Furthermore, the channel length assumed in the channel estimation is often limited due to complexity considerations for the estimation procedure and/or the symbol detection procedure. We now discuss appropriate MFBs when a reduced-order channel model is used. Two levels of suboptimality ensue in that case. These correspond to the two ways of implementing ML sequence estimation (MLSE) in the multichannel case: either use a vectorial matched filter and work with a scalar signal, or work with the vector received signal directly. These two strategies are only equivalent if the further processing of the scalar signal obtained in the first case is done in a specific way. Two measures corresponding to these two strategies are proposed.

We denote by  $\mathbf{H}_N(z)$  the full-order multichannel. Assume we have a reduced-order model  $z^{-d}\mathbf{H}_{N'}(z)$  of  $\mathbf{H}_N(z)$  ( $d \in \{0, 1, \dots, N-N'\}$ ,  $1 \leq N' \leq N$ ). In a first step of suboptimality, we can consider that in the data reduction step from multichannel to single channel, we use the MF matched to the reduced model  $z^{-d}\mathbf{H}_{N'}(z)$ . However, after this suboptimal data reduction, we shall allow optimal processing of the resulting single channel (this requires knowledge of  $\mathbf{H}_{N'}^\dagger(z)\mathbf{H}_N(z)$  which represents less information than  $\mathbf{H}_N(z)$  itself). In order to find the conventional MFB for the processing of the resulting scalar channel, it suffices to whiten the noise after the vector MF. The resulting scalar channel then indeed becomes one of additive white noise  $n(k)$  as indicated in Fig. 3 and becomes similar to Fig. 1(a) so that the MFB can be calculated as in Fig. 1(a). We get for the

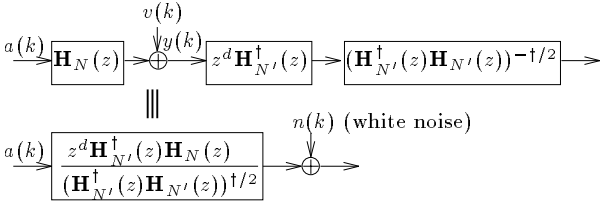


Figure 3: WMFB: reduced-order multichannel MF followed by a noise whitener.

continuous processing MFB:

$$\text{WMFB} = \frac{\sigma_a^2}{\sigma_v^2} \frac{1}{2\pi j} \oint \mathbf{H}_N^\dagger(z) \mathbf{P}_{\mathbf{H}_{N'}(z)} \mathbf{H}_N(z) \frac{dz}{z} \quad (9)$$

where  $\mathbf{P}_{\mathbf{H}(z)} = \mathbf{H}(z)(\mathbf{H}^\dagger(z)\mathbf{H}(z))^{-1}\mathbf{H}^\dagger(z)$ . Note that it is insensitive to the delay in the reduced order channel model.

It is interesting to analyze the variation of WMFB( $N'$ ) as a function of the reduced order  $N'$ . For  $N = N'$  we get  $\text{WMFB}(N) = \frac{\sigma_a^2}{\sigma_v^2} \|\mathbf{H}_N\|^2$ . It is not difficult to show that, in the limiting case  $N' = 1$  (purely spatial channel model), we get  $\text{WMFB}(1) = \frac{\sigma_a^2}{\sigma_v^2} \lambda_{\max}(\mathbf{H}_N^H \mathbf{H}_N)$ . We then can derive the following bounds

$$1 \leq \frac{\text{WMFB}(N)}{\text{WMFB}(1)} = \frac{\text{tr}(\mathbf{H}_N^H \mathbf{H}_N)}{\lambda_{\max}(\mathbf{H}_N^H \mathbf{H}_N)} \leq \min(m, N) \quad (10)$$

We see that a reduced-order model does not degrade WMFB a lot: in the case of 2 subchannels the maximal degradation will be a factor of 2, which could seem surprising when considering a purely spatial model only. The lower bound is attained when  $\mathbf{h}(i) \sim \mathbf{h}(0)$ ,  $i = 1, \dots, N-1$ . In that case,  $\mathbf{H}_N(z) = \mathbf{h}(0)\mathbf{H}_1(z)/h_1(0)$ . The spatio-temporal channel factors into spatial filter and a temporal one, and the optimal processing factors correspondingly: the full spatio-temporal treatment gets replaced by the cascade of a purely spatial combiner followed by a purely temporal treatment.

or  $\mathbf{H}_N^H \mathbf{H}_N \sim I_N$ , whichever is of full rank. In that case, the individual channel impulse responses are orthonormal. In a statistical set-up, if the  $m$  channel impulse responses are i.i.d., then the upper bound is approached as the delay spread grows.

Consider now the case of burst processing. Let  $\mathcal{T}_N$  and  $\mathcal{T}_{N'}$  denote  $\mathcal{T}_M(\mathbf{H}_N)$  and  $\mathcal{T}_M(\mathbf{H}_{N'})$  respectively and consider the Cholesky factorization  $\mathcal{T}_{N'}^H \mathcal{T}_{N'} = LL^H$ . Then the  $M+N'-1$  reduced-order WMF outputs are

$$L^{-1} \mathcal{T}_{N'}^H \mathbf{Y} = L^{-1} \mathcal{T}_{N'}^H \mathcal{T}_N A + L^{-1} \mathcal{T}_{N'}^H \mathbf{V} \quad (11)$$

The covariance matrix of the noise component is  $\sigma_v^2 I_{M+N'-1}$  while the covariance matrix of the signal part is  $\sigma_a^2 L^{-1} \mathcal{T}_{N'}^H \mathcal{T}_N \mathcal{T}_N^H \mathcal{T}_{N'} L^{-H}$ . The sum of the SNRs of all WMF outputs is then

$$\sum_{i=1}^{M+N'-1} \frac{\sigma_a^2}{\sigma_v^2} (L^{-1} \mathcal{T}_{N'}^H \mathcal{T}_N \mathcal{T}_N^H \mathcal{T}_{N'} L^{-H})_{ii} = \frac{\sigma_a^2}{\sigma_v^2} \text{tr}(\mathbf{P}_{\mathcal{T}_{N'}} \mathcal{T}_N \mathcal{T}_N^H) \quad (12)$$

This point of view corresponds to (a) in Fig. 2. To find the equivalent of (c) in Fig. 2, consider passing the previous WMF output  $L^{-1} \mathcal{T}_{N'}^H \mathbf{Y}$  through the scalar MF  $\mathcal{T}_{N'}^H \mathcal{T}_{N'} L^{-H}$ . This gives the  $M+N-1$  outputs

$$\mathcal{T}_N^H \mathbf{P}_{\mathcal{T}_{N'}} \mathbf{Y} = \mathcal{T}_N^H \mathbf{P}_{\mathcal{T}_{N'}} \mathcal{T}_N A + \mathcal{T}_N^H \mathbf{P}_{\mathcal{T}_{N'}} \mathbf{V} \quad (13)$$

As seen in section 2.2, the sum of the output SNRs in Fig. 2(c) is equal to the expression in equation (12). It is also possible to find the equivalent of (b) in Fig. 2, the sum of output SNRs giving again (12). What we call burst WMFB is again the average WMFB over the burst:

$$\text{WMFB} = \frac{1}{M+N-1} \text{tr}(\mathbf{P}_{\mathcal{T}_{N'}} \mathcal{T}_N \mathcal{T}_N^H) \quad (14)$$

### 3.2 ISI Canceler Matched Filter Bound (ICMFB)

We now go all the way in suboptimality. We will not only assume that the multichannel MF is based on the reduced channel model but in fact that the whole receiver is. To find the optimal performance in this case, consider MLSE. The received burst through the channel  $\mathbf{H}_N(z)$  is  $\mathbf{Y}_M(k) = \mathcal{T}_M(\mathbf{H}_N) A_{M+N-1}(k) + \mathbf{V}_M(k)$ . The channel estimation procedure has given a reduced-order model  $z^{-d}\mathbf{H}_{N'}(z)$  in which  $\mathbf{H}_{N'}(z)$  is known but the delay  $d$  may be unknown. Based on the reduced-order model  $z^{-d}\mathbf{H}_{N'}(z)$ , the MLSE problem is

$$\min_{a(i) \in \mathcal{A}} \|\mathbf{Y}_M(k) - \mathcal{T}_M(\mathbf{H}_{N'}) A_{M+N'-1}(k-d)\|^2 \quad (15)$$

$d \in \{0, 1, \dots, N-N'\}$

where  $\mathcal{A}$  is the symbol alphabet. We obtain the ISI Canceler Matched Filter Bound (ICMFB) by considering the detection of a single symbol  $a(i)$  assuming that the other symbols are known. It is easy to see that the continuous processing version of this leads to the structure in Fig. 4(a) (except

terms containing coefficients of the channel estimation error contribute to noise in the SNR computation. Hence, the equivalent structures in (b) and (c).

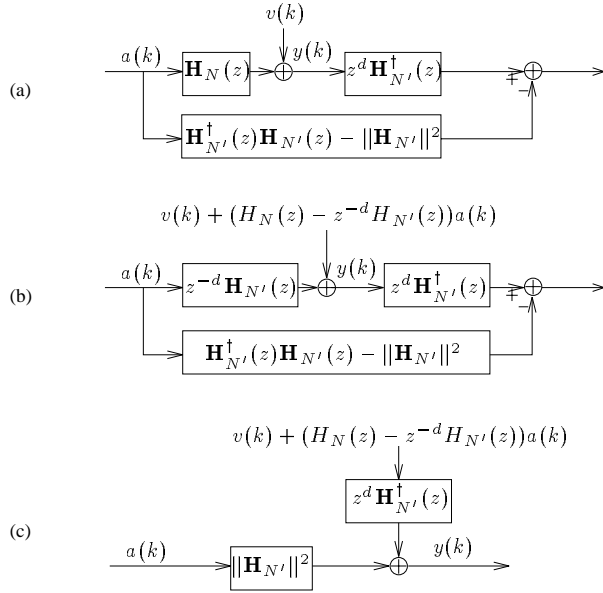


Figure 4: ICMFB: MFB for MLSE with the reduced-order channel model.

The output SNR in Fig. 4(c) is:

$$\text{ICMFB} = \max_{d \in \{0, \dots, N-N'\}} \frac{\|\mathbf{H}_{N'}\|^2 \sigma_a^2}{\sigma_v^2 - \sigma_a^2 \|\mathbf{H}_{N'}^\dagger(z)(z^d \mathbf{H}_N(z) - \mathbf{H}_{N'}(z))\|^2 / \|\mathbf{H}_{N'}\|^2} \quad (16)$$

In contrast to WMFB, the delay  $d$  in the reduced-order channel model plays a role in ICMFB. Note that the presence of an adjustable delay creates local minima for MLSE. Remark also that for  $N' = N$ , ICMFB=WMFB=MFB.

## 4 Two Applications

### 4.1 Deterministic Maximum Likelihood Channel Estimation

As a first example, we shall investigate the effect of model reduction in Blind Deterministic Maximum Likelihood (DML) Channel Estimation. A complete description of this method, which uses the IQML algorithm, is given in [1] and [2]. In [1], it is proven that, asymptotically, the DML criterion approximates the channel with a lower order model such that the output SNR of the Whitened Matched Filter corresponding to this lower order model gets maximized. Asymptotically, the reduced-order channel estimate obtained with the DML is the one that maximizes WMFB.

Some simulations were performed for  $m = 2$  channels and average SNR per subchannel of 10dB. In order to concentrate on the model reduction effects and not on the estimation errors, the averaged likelihood function was maximized. Blind methods only allow the estimation of the channel up to a multiplicative constant. WMFB on the other hand is

spirit of blind methods, we have determined the magnitude of this scale factor on the basis of the variance of the received signal, which leads to  $\|\mathbf{H}_{N'}\| = \|\mathbf{H}_N\|$ . The determination of the phase of the scale factor is less obvious though. In simulations we have avoided this issue by restricting to real impulse responses.

We considered continuous processing WMFB and ICMFB measures, but since the IQML method will normally be applied to a burst of data  $\mathbf{Y}_M(k)$ , we also considered the burst processing WMFB measure.

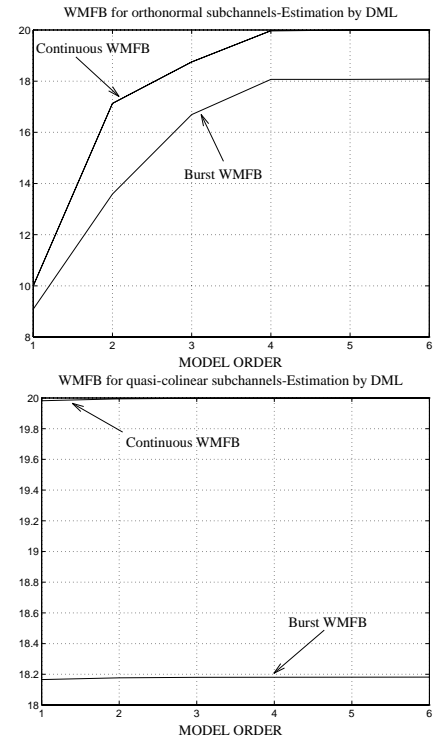


Figure 5: WMFB as a function of  $N' = 1, \dots, N$  for  $m = 2$ ,  $M = 50$ ,  $N = 6$  for orthonormal (left) and almost colinear (right) impulse responses.

First, we illustrate equation (10) where the minimal and maximal degradations when a model of reduced order 1 is considered are shown. Fig. 5 shows the evolution of the continuous and burst processing WMFB as a function of  $N'$  for a case in which the two impulse responses are orthonormal and a case in which they are almost colinear. In the first case, we see a degradation of approximately 1/2 from  $N' = N$  to  $N' = 1$  as predicted in (10). In the second case, quasi no degradations are visible. We note here that the burst WMFB is lower than its continuous processing version. This is due to the degradations occurring at the edges of the burst w.r.t. continuous mode performances.

Some other simulations were done for less particular channels. The evolution of WMFB and ICMFB as a function of

$$\mathbf{H}_1 = \begin{bmatrix} 1.0000 & 0.8000 & 0.5000 & 0.6000 & 0.1000 & 0.0050 \\ -1.5000 & 1.4000 & -0.9000 & 1.1000 & -0.0300 & 0.0050 \end{bmatrix}$$

$$\mathbf{H}_2 = \begin{bmatrix} 1.0000 & 0.5000 & -0.1500 & 0.0550 & 0.0145 & -0.0014 \\ 1.5000 & -0.9500 & 0.3050 & 0.0695 & 0.0431 & -0.0043 \end{bmatrix} \quad (17)$$

Both continuous and burst mode WMFB are plotted, as well as ICMFB.

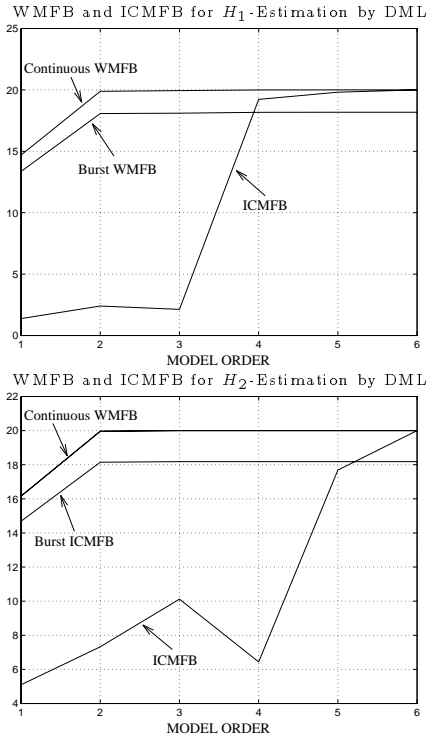


Figure 6: Comparison of WMFB and ICMFB as a function of  $N'$  for channels  $H_1$  and  $H_2$ ,  $m = 2$ ,  $N = 6$ ,  $M = 50$  in the case of DML estimation.

We notice that WMFB is greater than ICMFB for all reduced orders  $N'$ . The degradations due to reduced-order modeling are less severe for WMFB than for ICMFB, especially for low orders. This verifies equation (10), where we saw that maximal degradation for WMFB due to a model of reduced-order 1 is limited. Furthermore, degradations for WMFB occur mostly for  $N' = 1$ . As DML reduced-order models maximize WMFB, WMFB is decreasing as  $N'$  decreases.

For channel  $H_1$ , ICMFB decreases considerably when the reduced model is of order 3. This is probably due to the fact that the channel contains most of its energy in its first 4 coefficients, which shows that ICMFB is sensitive to the energy contained in the reduced-order channel.

#### 4.2 Training Sequence based Channel Estimation

In this second example, the channel is estimated by a white training sequence. The channel estimate of reduced-order

which contains the most energy. This estimation procedure produces a value for the delay  $d$ . However, this value for  $d$  may not be the best one for MLSE. Hence the problem formulation in (15) and the ensuing bound in (16) with optimization over  $d$  are still meaningful. Nevertheless, the optimal  $d$  thus obtained will usually equal the  $d$  obtained with channel estimation by training sequence.

We see in Fig. 7 that WMFB is not decreasing anymore, but remains high and always greater than ICMFB. Although training sequence based channel estimation does not maximize ICMFB, it tends to. Indeed, in equation (16), the numerator  $\|\mathbf{H}_{N'}\|^2$  gets maximized, and the coefficient in  $z^0$  of  $\mathbf{H}_{N'}^1(z)(z^d \mathbf{H}_N(z) - \mathbf{H}_{N'}(z))$  becomes equal to 0. In particular, we see how ICMFB improves, for channel  $H_2$  when the reduced-order channel is estimated by training sequence compared to DML estimation.

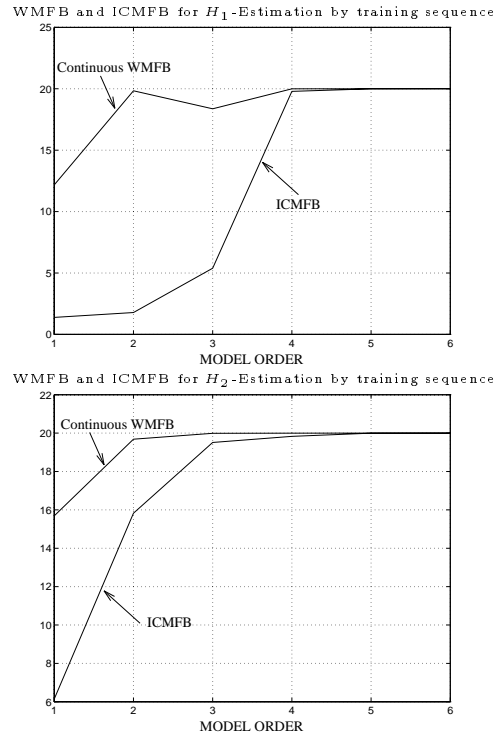


Figure 7: Comparison of WMFB and ICMFB as a function of  $N'$  for channels  $H_1$  and  $H_2$ ,  $m = 2$ ,  $N = 6$ ,  $M = 50$  in the case of training sequence based channel estimation.

#### References

- [1] E. de Carvalho and D. T. M. Slock. "Maximum-Likelihood Blind Equalization of Multiple FIR Channels". *To appear in Icassp'96*.
- [2] D.T.M. Slock and C.B. Papadias. "Further Results on Blind Identification and Equalization of Multiple FIR Channels". In *Proc. ICASSP 95 Conf.*, Detroit, Michigan, May 1995.